Journal of Alloys and Compounds 504S (2010) S376–S379

Contents lists available at ScienceDirect

Journal of Alloys and Compounds

journal homepage: www.elsevier.com/locate/jallcom

Preparation of Co/Ag nanocompound fluid using ASNSS with aid of ultrasonic orthogonal vibration

Ho Chang[a,*], Mu-Jung Kao[b], Ching-Song Jwo[c], Chin-Guo Kuo[d], Yu-Hsuan Yeh[a], Wei-Cheng Tzeng[a]

[a] Department of Mechanical Engineering, National Taipei University of Technology, No.1 Sec.3, Chung Hsiao E. Rd., Taipei 10608, Taiwan
[b] Department of Vehicle Engineering, National Taipei University of Technology, No.1 Sec.3, Chung Hsiao E. Rd., Taipei 10608, Taiwan
[c] Department of Energy and Air-Conditioning Refrigeration Engineering, National Taipei University of Technology, No.1 Sec.3, Chung Hsiao E. Rd., Taipei 10608, Taiwan
[d] Department of Mechatronic Technology, National Taiwan Normal University, No.1 Sec.1, Ho-Ping E. Rd., Taipei 10610, Taiwan

ARTICLE INFO

Article history:
Received 18 June 2009
Received in revised form 16 April 2010
Accepted 19 April 2010
Available online 16 May 2010

Keywords:
Co/Ag nanocompound fluid
Magnetization
Coercivity
Heat transfer coefficient

ABSTRACT

This article describes an arc-submerged nanofluid synthesis system (ASNSS) using ultrasonic orthogonal vibration that was developed to fabricate Co/Ag nanocompound fluid. In the fabrication process, the positive electrode of an Ag rod and the ultrasonic vibrator are combined to form an orthogonal model with the negative electrode of a Co rod. The two electrodes are then installed inside the vacuum chamber, with deionized water as the dielectric liquid. This nanocompound fluid is analyzed by morphological analysis, heat transfer analysis, magnetism analysis and suspension stability. The experimental results show that the nanocompound fluid is composed of Co, Ag and Co_3O_4, and the mean particle size is 30 nm. The pH value of the prepared nanocompound fluid is 3.8, and the Zeta potential is 31 mV, so the prepared nanofluid has excellent suspension stability. For the heat transfer experiment, the experimental ambient temperature is 40 °C, weight concentration is 0.4%, and average heat transfer coefficient is 0.79 W/m °C. The magnetism test shows that the saturation magnetization of the produced Co/Ag nanocompound fluid is 5.213 emu/g, the saturation magnetic strength is 6666.93 Oe, the coercivity is 56.62 Oe and the remanent magnetization is 0.0945 emu/g.

1. Introduction

The application and technological development of nanocomposite and nanocompound materials have recently grown rapidly in engineering industries and academic fields. In recent years, considerable efforts have been devoted to the design and controllable preparation of different kinds of nanocomposite particles with different morphologies owing to their superior properties compared with conventional composite materials and potential applications in various fields, such as optics, catalysis, magnetism, antibiotic and medicines [1–6].

Silver nanoparticles have attracted particular interest due to their favorable optical properties, including surface plasma resonance, non-linear optical limitation, and the ability to modify the refractive index of host materials [7]. Furthermore, silver particles have been widely used to form conducting pastes for integrated circuits and other electronic devices [8]. The quality of the pastes depends mostly on the properties of the metal particles such as monodispersity, sphericity, dispersion without agglomeration, purity and crystallinity [9].

Magnetic nanocomposites have many possible technological applications [10]. Shi assigned cobalt ferrite nanoparticles prepared by a combination of chemical precipitation, mechanical alloying and subsequent heat treatment [11]. In that study, sodium chloride was added before milling in order to avoid agglomeration, and TEM measurements showed that the nanoparticles had a fairly uniform structure with a mean particle size of approximately 10 nm. Anisotropic nanoparticles were obtained after magnetic annealing at 300 °C. Experimental results showed that the Co powders demonstrated ferromagnetic behavior [12]. Some co-related studies to magnetic nanocomposite materials like Bradley who developed theoretical model for the description of the effects of displacement reactions on the composition of pulse-plated binary alloys has been successfully applied to copper–cobalt alloys [13]. Hillier and Robinson used slow strain rate tests to perform on quenched and tempered AISI 4340 steel to measure the extent of hydrogen embrittlement caused by electroplating with zinc–cobalt alloys [14]. Kyomoto et al. created a highly lubricious metal-bearing material: A 2-methacryloyloxyethyl phosphorylcholine (MPC) polymer was grafted onto the surface of the cobalt–chromium–molybdenum (Co–Cr–Mo) alloy [15]. Mani et al., for the first time, reported the formation and stability of self-assembled monolayers (SAMs) on a Co–Cr–W–Ni alloy. SAMs of octadecyltrichlorosilanes (OTS) were coated on sputtered

* Corresponding author. Tel.: +886 2 27712171x2063; fax: +886 2 27317191.
E-mail address: f10381@ntut.edu.tw (H. Chang).

0925-8388/$ – see front matter © 2010 Elsevier B.V. All rights reserved.
doi:10.1016/j.jallcom.2010.04.127

Co–Cr–W–Ni alloy thin film and bulk Co–Cr–W–Ni alloy [16]. Cavallotti et al. reported the results on electrodeposition of Co–Pt–W (P) and Co–Pt–Zn (P) layers from sulphamate citrate solutions [17]. Su et al. described the magnetic properties of highly ordered $Fe_{48}Co_{52}$ alloy nanowire arrays with different interpore distances and diameters were found to change differently after annealing [18]. Li et al. fabricate the $Co_{49}Pt_{51}$ nanowire arrays with an average diameter of 35 nm and lengths up to several micrometers were grown in an ordered porous anodic aluminum oxide (AAO) template using direct-current electrodeposition [19].

Most of these studies treat Ag nanocomposites or Co nanocomposites, such as ZnO/Ag, Co/Fe, Ni/Ag, and Co/TiN; but Co/Ag nanofluid has not yet been studied [9,20–22]. Silver has the advantages of good conductivity, thermal conductivity, inoxidizability and significant antibacterial effects. Co belongs to magnetic materials and Co nanoparticles can serve as the carrier of medicament. This paper expects to prepare for Co/Ag nanocompound particles with antibacterial and magnetic properties to conjugate with different sequence of DNA to apply to biomedical domains in future study. Therefore, this paper explores the material properties of Co/Ag nanocompound fluid. We analyze the distribution, size and shape of nanoparticles with particle size analyzer and SEM, the components of particles with XRD, the magnetic property of particles with SQUID. We also analyze the thermal conductivity [23], Zeta potential of fluids, and the influence of pH value on Zeta potential.

2. Experimental

We constructed a nanocompound fluid with an arc-submerged nanofluid synthesis system (ASNSS) using of ultrasonic orthogonal vibration, in which the positive electrode with an Ag rod and the ultrasonic vibrator are combined to form an orthogonal model having the negative electrode of a Co rod (purity of each is 99.9%). The experimental device is comprised mainly of a heating system, an ultrasonic orthogonal vibration system, a pressure control system, and a temperature control system [24,25]. Ultrasonic orthogonal vibration produces alternating pressure variations which lead to increased hydrostatic pressure variation. In addition, the ultrasonic orthogonal vibration system allows different frequency settings (19.2–25.8 kHz). With the help of ultrasonic vibration, the disturbance of the dielectric liquid can be increased and the nanoparticles thus produced can easily move away from the fusion zone and be cooled down quickly by the low-temperature coolant surrounding it [26,27]. Secondary particle size analysis indicates that 45 nm is the average particle size. The fabricated Ag/Co nanocompound fluid is immediately allowed to dry and the dried powder is attached to a standard test plate with petrolatum vaseline for XRD component analysis. Then field emission scanning electron microscope (FE-SEM) is used to analyze nanoparticle shape.

To analyze magnetic property, we dry the nanocompound fluid into a powder and put it into capsule container with magnetic field intensity set at -10^4 to $+10^4$ Gauss and temperature of 25 °C. Then the magnetic character of the powder is analyzed to obtain the hysteresis loop of the nanocompound fluid. In addition, 0.1 M HCL and 0.1 M NaOH are used to formulate the pH value of the fluid so as to observe the influence of fluid pH value on nanoparticles, and draw the relationship between pH and Zeta potential.

To determine the heat transfer coefficient, we first dry the fluids into powders, which are mixed with deionized water to achieve the intended concentration, and then analyze the mixture with a Decagon KD2 Thermal Properties Analyzer. The weight concentrations of the fluids fabricated in this experiment are 0.05%, 0.1%, 0.2% and 0.4%. Before analysis, the fluid is placed in a constant temperature cistern until it achieves the expected temperature. The temperature is set at 10 °C, 20 °C, 30 °C and 40 °C, and at each data point we conduct experiments 10 times and obtain the average value so as to reduce error. The resulting data are shown in Table 1.

3. Results and discussion

Fig. 1 shows the FE-SEM image of the prepared Co/Ag nanocompound particles and most of which are more spherical forms. The results obtained in XRD component analysis are shown in Fig. 2, which shows the XRD pattern of the Co/Ag nanocompound fluid. By comparing the XRD pattern after examination with the standard spectrum from a JCPD card, it can be seen that the crystal structures of the fabricated particles are Co, Ag and Co_3O_4, as shown in Fig. 2. The pH value of the prepared Co/Ag nanocompound fluid is 3.8. During the preparation process, the Co_3O_4 nanoparticles came from the decomposed salt (Co_2^+) in the solution (pH < 7). In addition, there existed little Ag nanoparticles in the prepared nanofluid system by electrochemical reaction, and the Co nanoparticles came more likely from tiny dissolution.

Table 1
Data sheet of heat transfer coefficients for Co/Ag/Co_3O_4 nanocompound fluid.

	Temperature			
	10 °C	20 °C	30 °C	40 °C
	(Heat transfer coefficient, W/m °C)			
0 wt%	0.570	0.594	0.608	0.639
0.05 wt%	0.575	0.605	0.641	0.672
0.1 wt%	0.580	0.619	0.666	0.698
0.2 wt%	0.587	0.640	0.700	0.742
0.4 wt%	0.595	0.666	0.737	0.790

Fig. 3 shows the magnetic properties of the powder with average particle size of 30 nm. It can be seen from Fig. 3 that the prepared Co/Ag nanocompound particles are ferromagnetic with the coercivity value of 56.62 Oe, and the saturation magnetization intensity is 666.93 Oe. The saturation magnetization of prepared nanocompound particles is 5.213 emu/g, and the remanent magnetization is 0.0945 emu/g.

Fig. 4 shows that when the fabricated Co/Ag nanocompound fluid has a pH value of about 10, the particle's Zeta potential is zero, which is called the isoelectric point (IEP). However, when its

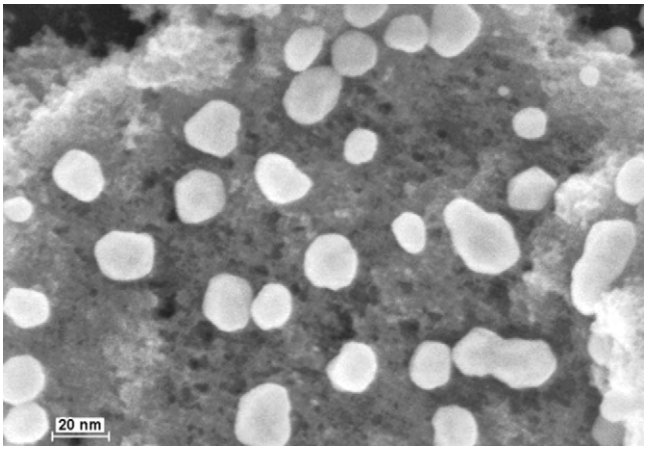

Fig. 1. FE-SEM image of the prepared Co/Ag/Co_3O_4 nanocompound particles.

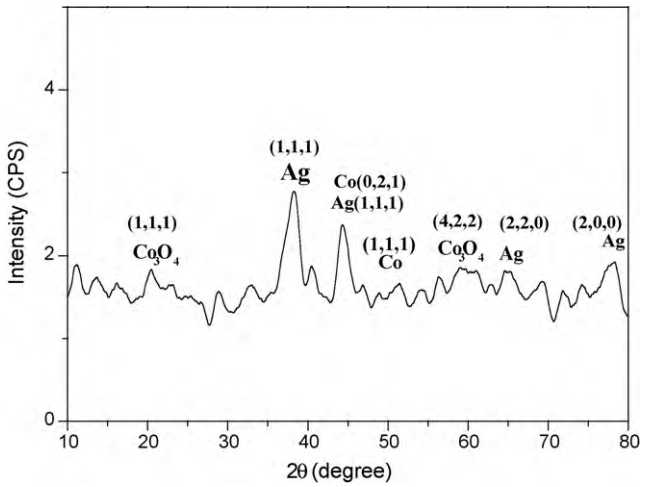

Fig. 2. XRD pattern of Co/Ag nanocompound fluid.

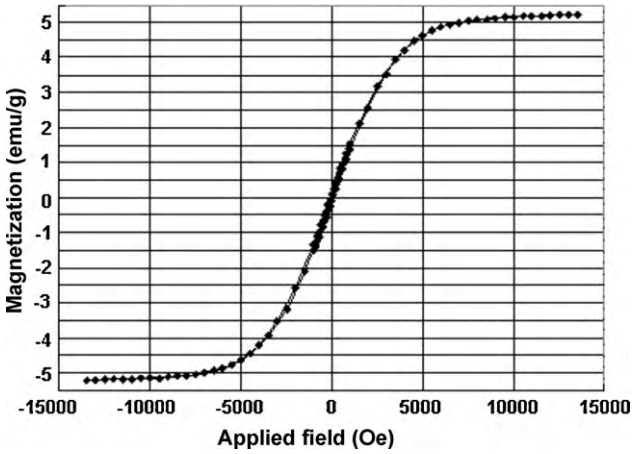

Fig. 3. Hysteresis curve of the prepared nanocompound fluid.

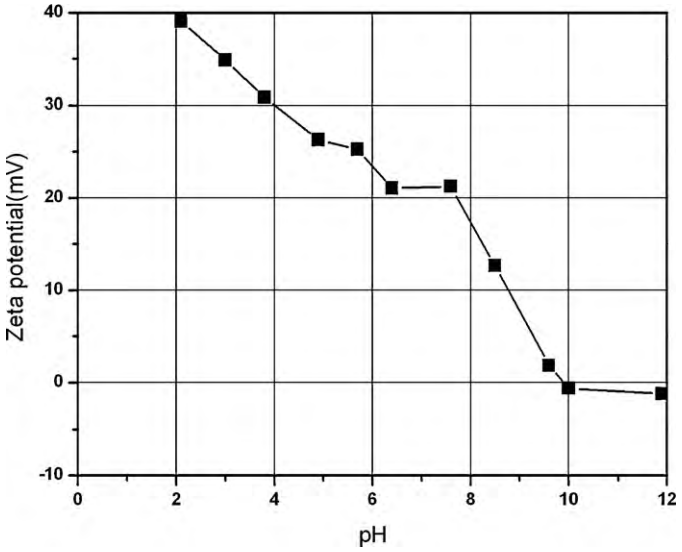

Fig. 4. Relationship between pH value and Zeta potential.

pH value is higher than 10, the particle surface begins to carry a negative charge. In contrast, when its pH value is lower than 10, the particle surface begins to carry a positive charge. The Co/Ag nanocompound fluid fabricated in our experiment has a pH value of 3.8 and a Zeta potential of 31 mV and fairly good suspension. With the help of ultrasonic orthogonal vibration, the disturbance of the dielectric liquid can be increased and the nanoparticles thus produced can quickly come out of the fusion zone. In the meantime, the gasified metal can be quickly cooled down. Furthermore, the

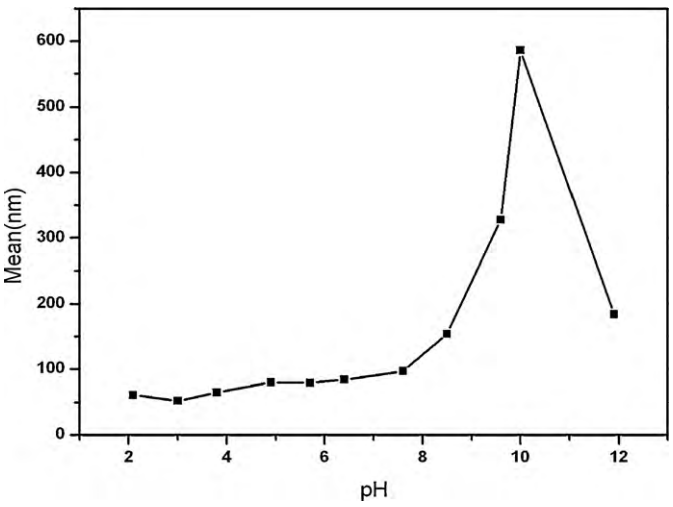

Fig. 5. Relationship between pH value and mean particle size.

ultrasonic orthogonal vibration of the electrode prevents sedimentation of nanoparticles in the working gap and yields an animated suspension in the deionized water, which improves the water circulation. The prepared Co/Ag nanocompound fluids already have good dispersion; and even without dispersant, they can still remain in stable suspension for a fairly long time.

The influence of pH value on particle size of the Co/Ag nanocompound fluid is shown in Fig. 5. As this figure shows, before pH value reaches 6.2, the secondary particle size of Co/Ag nanocompound fluid reaches nanoscale with good fluid suspension. However, when pH value is 6.2, it displays a phenomenon of particle flocculation occurs and the particles gather at the bottom. When pH value exceeds 7.8, particles show substantial gathering and precipitation; especially when pH value reaches 10, at which point the fluid displays almost no suspension, but only coagulation and precipitation. Fig. 6(a) shows the results of SEM analysis when pH value is 10, and Fig. 6(b) shows the even distribution of particles when pH value is 5.5.

Table 1 shows the relationship between weight concentration and heat transfer coefficient. It can be seen from Table 1 that when adding Co/Ag nanocompound fluid and increasing the temperature, the heat transfer coefficient also increases accordingly. Furthermore, the average heat transfer coefficient of Co/Ag nanocompound fluid is 0.79 W/m °C at the conditions of ambient temperature of 40 °C and weight concentration of 0.4%.

With the four variables of nanofluid concentration between 0.05 and 0.4 wt%, as shown in Fig. 7, and with temperature set at 10 °C, the thermal conductivity of the experimental sample increases from 0.9% to 4.3%; at 20 °C the thermal conductivity increases from 1.9% to 12.1%; at 30 °C the thermal conductivity increases from 5.4%

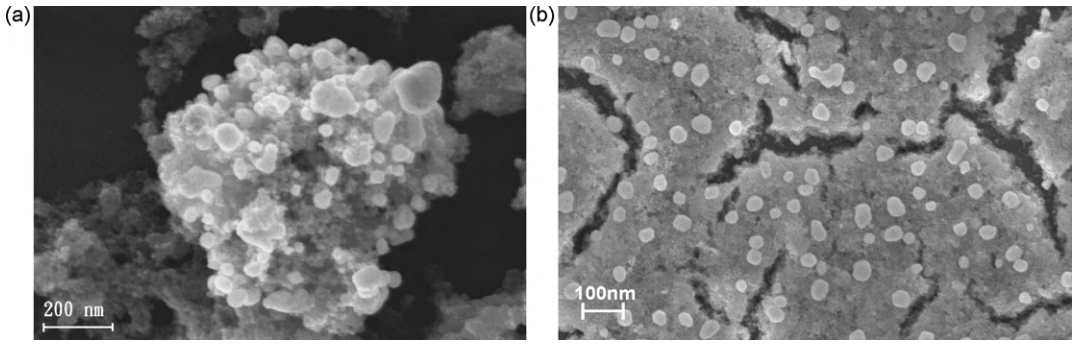

Fig. 6. (a) pH 10, (b) pH 5.5, FE-SEM image of Co/Ag/Co_3O_4 nanocompound particles.

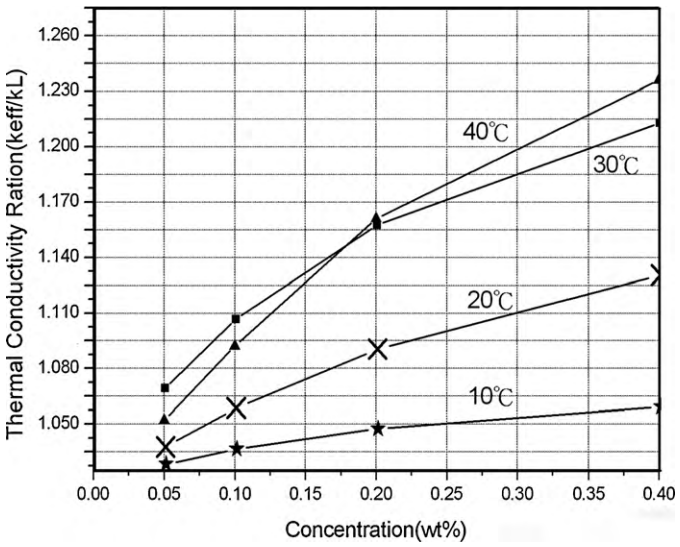

Fig. 7. Relationship between weight concentration and thermal conductivity ratio for different temperatures.

to 21.2%; and set at 40 °C, the average heat transfer coefficient is 0.79 W/m °C and the thermal conductivity increases from 5.6% to 23.6%. Thus, under the same temperature variation, with higher experimental sample concentration, the thermal conductivity ratio increase is more obvious. In other words, there is better performance at higher temperature. Overall, with higher concentration of added nanoparticles, the thermal conductivity ratio increase is more obvious, which is in agreement with previous research [28]. Temperature not only affects the heat transfer coefficient but also changes the thermal conductivity of nanoparticles. This is because the rate of particle movement is changed by temperature, which in turn changes the probability of particle impact. With higher temperatures, the particle impact is quicker and the thermal conductivity is higher, and vice versa. When the particles are smaller, the reaction is more noticeable since it requires less kinetic energy.

4. Conclusions

From these results and discussions, we propose the following three conclusions concerning the Co/Ag nanocompound fluid fabricated with ASNSS:

1. Ultrasonic orthogonal vibration can effectively improve the dispersion of the prepared Co/Ag nanocompound suspension.
2. The Co/Ag nanocompound fluid had an i.e.p. of 10. When the pH value of the suspension fluid is lower than 6.2, the Co/Ag nanocompound particles become stably suspended.
3. With temperature set at 40 °C and weight concentration set at 0.4%, the heat transfer coefficient for the prepared Co/Ag nanocompound fluid is 0.79 W/m °C, an increase of 23.6%.
4. Magnetic examination shows that the coercivity of the prepared Co/Ag nanocompound fluid is 56.62 Oe and remanent magnetization is 0.0945 emu/g. In addition, the hysteresis curve indicates that the prepared Co/Ag nanocompound fluid is ferromagnetic.

Acknowledgement

This study was supported by the National Science Council of Taiwan, Republic of China under grant NSC 9×6-2212-E-027-093.

References

[1] Y. Wu, Y. Zhang, J. Xu, M. Chen, L. Wu, J. Colloid Interface Sci. 343 (2010) 18–24.
[2] E.J. Bourgeat-Lami, Nanosci. Nanotech. 2 (2002) 1–24.
[3] S. Kidambi, J.H. Dai, M.L. Bruening, J. Am. Chem. Soc. 126 (2004) 2658–2659.
[4] H. Xu, L.L. Cui, N.H. Tong, H.C. Gu, J. Am. Chem. Soc. 128 (2006) 15582–15583.
[5] M. Zhang, G. Gao, D.C. Zhao, Z.Y. Li, F.Q. Liu, J. Phys. Chem. B 109 (2005) 9411–9415.
[6] X.J. Zhang, R.P. Bagwe, W.H. Tan, Adv. Mater. 16 (2004) 173–176.
[7] K.L. Kelly, E. Coronado, L.L. Zhao, G.C. Schatz, J. Phys. Chem. B 107 (2003) 668–677.
[8] O.K. Choi, Z.Q. Hu, Water Sci. Technol. 59 (2009) 1699–1702.
[9] S.Y. Yang, S.G. Kim, Powder Technol. 146 (2004) 185–192.
[10] R.W. Cahn, Nature 359 (1992) 591–592.
[11] Y. Shi, J. Ding, H. Yin, J. Alloys Compd. 308 (2000) 290–295.
[12] S. Wu, S. Zhang, W. Huang, J. Shi, B. Li, Y. Suns, J. Mater. Sci. Technol. 19 (2003) 422–424.
[13] P.E. Bradley, D. Landolt, Electrochim. Acta 45 (1999) 1077–1087.
[14] E.M.K. Hillier, M.J. Robinson, Corros. Sci. 46 (2004) 715–727.
[15] M. Kyomoto, Y. Iwasaki, T. Moro, T. Konno, F. Miyaji, H. Kawaguchi, Y. Takatori, K. Nakamurad, K. Ishiharab, Biomaterials 28 (2007) 3121–3130.
[16] G. Mani, M.D. Feldman, S. Oha, C.M. Agrawal, Appl. Surf. Sci. 255 (2009) 5961–5970.
[17] P.L. Cavallotti, M. Bestetti, S. Franz, Electrochim. Acta 48 (2003), 3013-/3020.
[18] H.L. Su, G.B. Ji, S.L. Tang, Z. Li, B.X. Gu, Y.W. Du, Nanotechnology 16 (2005) 429–432.
[19] H. Li, C.L. Xu, G.Y. Zhao, H.L. Li, J. Phys. Chem. B 109 (2005) 3759–3763.
[20] J. Jose, M.A. Khadar, Acta Mater. 49 (2001) 729–735.
[21] A. Basumalick, K. Biswas, S. Mukherjee, Mater. Lett. 30 (1997) 363–368.
[22] Y. Sakka, S. Ohno, Appl. Surf. Sci. 100 (1996) 232–237.
[23] W.A. Wakeham, J.V. Sengers, Measurement of the Transport Properties of Fluids, Oxford, Blackwell, 1991.
[24] H. Chang, T.T. Tsung, C.H. Lo, H.M. Lin, C.K. Lin, C.S. Jwo, J. Mater. Sci. 40 (2005) 1005–1010.
[25] H. Chang, Y.C. Wu, M.J. Kao, T.J. Shieh, C.S. Jwo, J. Vac. Sci. Technol. B 27 (2009) 1381–1384.
[26] J.C. Ball, R.G. Compton, Electrochemistry 67 (1999) 912–919.
[27] J. Zhijin, Z. Jinianhua, A. Xing, Int. J. Mach. Tool Manuf. 37 (1997) 193–199.
[28] S.K. Das, N. Purtra, P. Thiesen, Roetzel, ASME J. Heat Transfer 125 (2003) 567–574.